

## Review

# The Mechanical Behavior of High-Strength Concrete-Filled Steel Tubes: A Review

Clemente Pinto \*  and João Fonseca

Centre of Materials and Civil Engineering for Sustainability (C-MADE), Department of Civil Engineering and Architecture, University of Beira Interior, Calçada Fonte do Lameiro Edifício II das Engenharias, 6201-001 Covilhã, Portugal; jfonseca@ubi.pt

\* Correspondence: cmp@ubi.pt

**Abstract:** This review explores the mechanical behavior of high-strength concrete-filled steel tubes (CFSTs), focusing on their structural integrity and failure mechanisms. This study highlights the crucial role of the steel tube in providing passive confinement, which limits crack progression and enhances the ductility of the concrete. The concept of concrete as a structural system composed of micro- and mini-pillars, derived from rock mechanics, can be a useful approach to understanding CFST behavior. The review identifies that the strength index (SI) can, in some cases, decrease with an increase in the confinement factor ( $\xi$ ), particularly in high-strength and ultrahigh-strength concrete (HSC and UHSC), which seems to be different to the common understanding of confinement. The experimental results show that different crack patterns and concrete compositions significantly impact the CFST performance. For example, silica fume in concrete mixtures can reduce the strength enhancement despite increasing the unconfined compressive strength. This work advocates for a mechanistic approach to better comprehend the interaction between concrete and steel tubes, emphasizing the need for optimized concrete mixtures and improved mechanical interaction. Future research should focus on the potential of HSC and UHSC in CFST, addressing factors such as crack progression, confinement effects, and concrete–steel interaction.

**Keywords:** concrete-filled steel tubes (CFST); compression behavior; confinement; failure mode; microcracks; high-strength concrete (HSC)



**Citation:** Pinto, C.; Fonseca, J. The Mechanical Behavior of High-Strength Concrete-Filled Steel Tubes: A Review. *CivilEng* **2024**, *5*, 591–608. <https://doi.org/10.3390/civileng5030032>

Academic Editor: Angelo Luongo

Received: 23 May 2024

Revised: 4 July 2024

Accepted: 23 July 2024

Published: 31 July 2024



**Copyright:** © 2024 by the authors. Licensee MDPI, Basel, Switzerland. This article is an open access article distributed under the terms and conditions of the Creative Commons Attribution (CC BY) license (<https://creativecommons.org/licenses/by/4.0/>).

## 1. Introduction

In recent years, concrete-filled steel tubes (CFSTs) have been used in different structural applications [1,2]. Particularly in China, CFST solutions have been a frequent option to construct long-span arch bridges [1,3]. Additionally, CFST solutions are applied in high-rise buildings [2]. In structures where a high compressive bearing capacity is needed, CFST solutions are adequate. It is well known that the transversal confinement of concrete increases the compressive strength and ductility, which effectively occurs in CFST solutions. CFSTs exhibit enhanced strength and ductility due to the combined effect of the concrete and steel tubes. The reciprocal effect between the concrete and the steel tube in CFSTs improves the mechanical properties of the structure. The concrete is confined in a steel tube, and it reinforces the steel tube due to local buckling. The strength enhancement observed in normal-strength concrete (NSC) is comparatively more significant than that observed in high- and ultrahigh-strength concrete (HSC and UHSC). The potential of CFSTs to achieve the structural requirements under high-loading conditions and the high demands of ductility has motivated and justified diverse research to understand and improve the behavior of CFSTs. The effects of different parameters, such as the concrete strength, the  $D/t$  ratio of the tubes, the slenderness, the loading application mode, and additional ways to achieve more confinement have been studied in many works [4–17]. Generally, there is consensus that the tube effect increases the concrete compressive strength and, more significantly, the ductility. The use of external reinforcement beyond the tubes also improves the behavior,

especially of the ductility, a critical requirement for seismic conditions. However, according to experimental results, an increase in the confinement effect of the steel tube does not always increase the load-bearing capacity of concrete [4–6]. This observation demonstrates an inconsistency with the conventional concept of confinement.

Much of the research on CFST solutions is based on FEM modeling. FEM modeling and analysis has provided significant contributions to the scientific development of CFSTs. However, there are some limitations and needed improvements. As an example, one could refer to [17], a detailed Ph.D. thesis about concrete confined with external thin circular tubes. In fact, the modeling and failure theories for concrete were able to predict the loading capacity and the failure mode of the concrete inside the tube. However, the analysis was not able to predict and simulate the diagonal fracturing of the external steel tube, as clearly stated by the author. This exemplified limitation, the inconsistencies of some observed experimental results, and the expected application of complex prediction models, justify a review based on the mechanical destruction processes of concrete, as conducted in this research.

Under compressive loading, concrete suffers cracks, even inside a steel tube. Thus, an attempt to understand the mechanical behavior of the CFST solutions needs to account for the effects of cracks, which will depend on their progression, distribution, and number. From a more global perspective, brittle materials under compression loading should be considered as structural systems characterized by the presence of micro- and mini-pillars between cracks [18]. Based on this concept, confined and unconfined concrete are different systems because the progression of cracks is different and, consequently, so too is the structural system.

Understanding the failure modes has a crucial role in determining the mechanical behavior of concrete in confined conditions such as in CFSTs. The failure modes can be related to the crack pattern of the concrete, describing indirectly what occurs inside the tube. The idea of a structural system, formed by micro-pillars between cracks, gives a mechanistic rationale to the description. Parameters such as the concrete composition, the shape and dimensions of the specimens, the stiffness of the loading system, the loading application mode, and the interaction between concrete and tubes, which affect the failure mode and load-bearing capacity of the structural systems, including CFSTs, can be accounted for in the analysis. Knowledge about the processes of cracking, the crack progression, and failures is needed. The similarities between high-strength concrete and high-strength rocks [19,20], as brittle materials with complex internal structure, justify the use of rock mechanics knowledge [21–30].

Design codes for CFSTs account for the confinement effect using different formulations [31]. For example, Eurocode 4 [31–33], as a reference for this work, accounts for the confinement effect when the relative slenderness ratio is lower than 0.5 and considers the eccentricity of the applied loading, which is equal to zero in uniform compression. It also considers the ratio between the tube thickness and diameter, as well as the ratio between the yield strength of steel and the compressive strength of concrete. These formulations (1)–(6) consider that the confinement decreases with a higher column slenderness and loading eccentricity, which means bending effects. Thus, to evaluate the confinement effects, compact columns are preferable.

$$N_{Rd} = \eta_s A_s f_y + \left( 1 + \eta_c \frac{t_s}{D} \frac{f_y}{f_c} \right) \quad (1)$$

$$\eta_s = 0.25(3 + 2\bar{\lambda}) \leq 1.0 \quad (2)$$

$$\eta_c = 4.9 - 18.5\bar{\lambda} + 17\bar{\lambda}^2 \geq 0 \quad (3)$$

$$\bar{\lambda} = \sqrt{\frac{f_c A_c + f_y A_s}{N_{cr}}} \quad (4)$$

$$N_{cr} = \frac{\pi^2 EI_{eff}}{l^2} \quad (5)$$

$$EI_{eff} = E_s I_s + 0.6 E_c I_c \quad (6)$$

Different researchers have conducted analyses of design code applications based on experimental results and numerical simulations [5,11,12,34]. According to [11], Eurocode 4 provides nonconservative results with relative slenderness ratios lower than 0.4 and conservative results for relative slenderness ratios higher than 0.4. In the tests, they considered concrete compressive strengths of 56, 66, and 107 MPa. A similar trend was found in [9].

The conclusions of [5] show that Eurocode 4 provides good predictions for ultrahigh-strength short circular CFST columns. However, the authors of [5] also proposed an alternative formula for ultrahigh-performance-concrete-filled steel tubes, which takes in to account the diameter-to-thickness ratio and the steel yield strength to 235 MPa ratio. Based on experimental tests with compressive-strength concrete ranging between 140 and 184 MPa, the analysis presented in [12] shows that Eurocode 4 overestimated the confinement effect, which should be ignored.

The references above show that the different codes provide different results, concerning the underestimation or overestimation of the loading capacity. Concerning Eurocode 4, it seems relevant that an overestimation of the loading capacity appears for lower slenderness values. Taking into consideration that the slenderness implies failure modes with bending effects and even buckling, in which confinement action is not achieved, the limitations for the Eurocode 4 seem to be related to the inadequate accounting/understanding of the interaction between concrete and steel tubes.

The need for material consumption optimization with adequate behavior in extreme events, such as earthquakes, justifies the attempts to better understand how concrete and, particularly, high-strength concrete, work inside the steel tubes. The approach proposed in this work, based on the internal destruction processes of concrete, similar to other brittle materials, aims to mitigate the inconsistencies and limitations of the codes and computational analyses.

## 2. Survey of the Experimental Results

### 2.1. Quantitative Parameters

Two parameters were considered for the quantitative analysis of CFST elements, following the procedure adopted in different references, such as [4–12]: (i) the strength index SI (7), which evaluates the compressive strength gain of the filling concrete due to the confinement effect of the steel tube, and (ii) the confinement factor  $\xi$  (8), which is the ratio between the strength of the steel tube and the concrete core.

$$SI = \frac{Nu}{f_y A_s + f_c A_c} \quad (7)$$

$$\xi = \frac{f_y A_s}{f_c A_c} \quad (8)$$

Figure 1 depicts the relationship between the strength index and the compressive strength of concrete. The values were obtained from previous studies [4–11]. The results demonstrated that higher strength index (SI) values were observed for NSC. Conversely, lower SI values were obtained for HSC and UHSC. This observation is typical for confined concrete, and it is also observed when fiber-reinforced polymers (FRP) elements are used [27–29]. However, a distortion in the SI values can be observed for the same values of compressive strength, which indicates that the compressive strength does not determine the mechanical behavior of the CFST elements. Figure 2 shows the relationship between the strength index SI and the confinement factor ( $\xi$ ). It can be observed that the strength index increases with an increase in the confinement factor. However, similar to the case above, a distortion in the SI values was observed for the same values of the confinement factor.

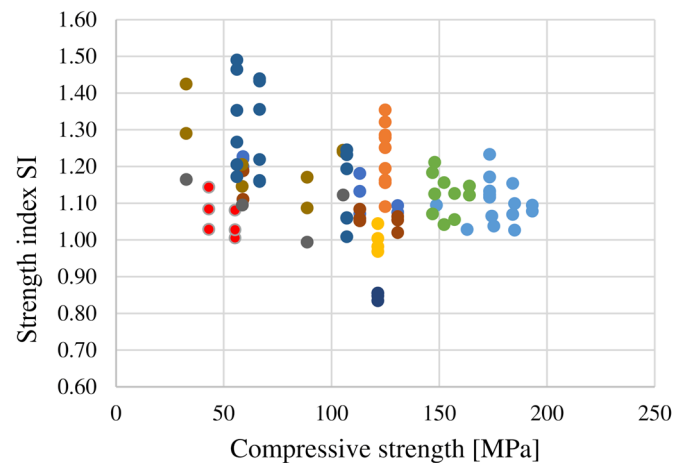


**Figure 1.** Relation between the strength index (SI) and the concrete compressive strength, according to references [4–11].

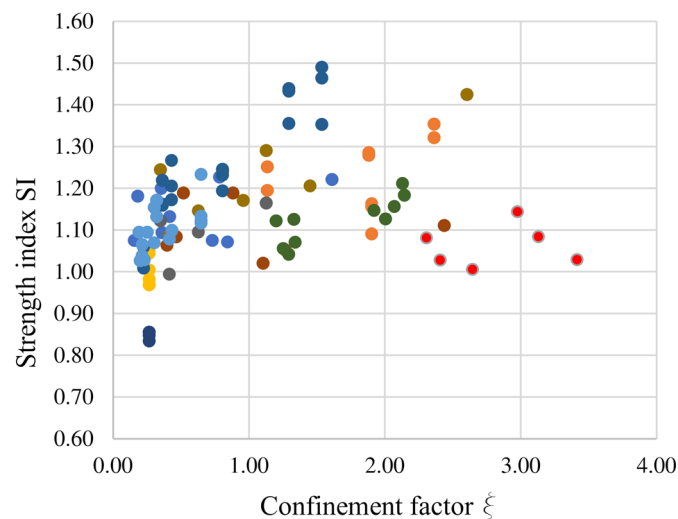


**Figure 2.** Relation between the strength index and the confinement factor, according to references [4–11].

A separate analysis of the data in Figure 2 can be performed to obtain relevant results. Figures 3 and 4 depict the results obtained from [5]. The relationship between the strength index and the confining factor for circular and square sections and different values of the concrete compressive strength can be observed in these figures. The strength index value decreased with an increase in the confinement factor, which is inconsistent. Similar results were described in [6,7]. It was hypothesized that this behavior was observed due to the variation in the cross-sectional dimensions [6], the local buckling of the steel tube, and the utilization of the high compressive strength of concrete [7]. However, in [5], different values of the confinement factor were obtained by varying the tube thickness while maintaining constant cross-sectional dimensions. Additionally, the same behavior was observed for a concrete specimen with a low compressive strength (59 MPa). The presence of steel fibers in the composition of concrete, described in [5], affected the concrete specimens with a compressive strength of 113 and 131 MPa. The two concrete mixes had different proportions of steel fibers (0.22 and 0.05) and superplasticizers (0.04 and 0.05), respectively. The results shown in Figure 3 demonstrated that the CFST elements with concrete containing a higher proportion of steel fibers exhibited a significant decrease in the strength index value with an increase in the confinement factor ( $\xi$ ).

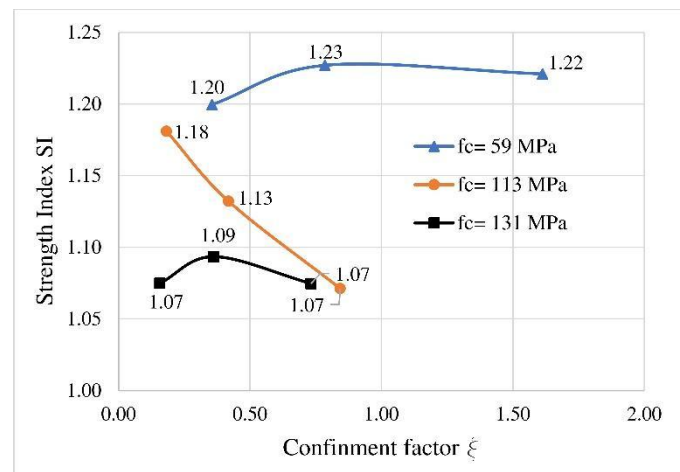


**Figure 3.** Relation between the strength index and the confinement factor obtained in the experimental tests of circular sections, described in [5] (adapted).

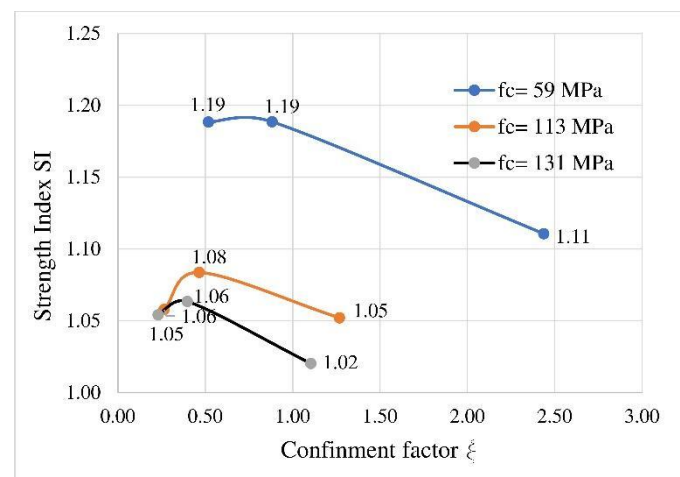


**Figure 4.** Relation between the strength index and the confinement factor obtained in the experimental tests of square sections, described in [5] (adapted).

The relationship between the strength index and the confinement factor values obtained [9,10] is depicted in Figure 5. The load was applied to the cross section of concrete and steel in [9]. In contrast, only concrete was loaded for the compression tests conducted in [10]. Coarse aggregates ( $D_{max} = 19$  mm) were used in the tested concretes, with compressive strengths of 30, 60, 80, and 100 MPa. Silica fume was used in the two concrete specimens with high compressive strength. The studies [5,9,10] demonstrated the same level of concrete compressive strength (approximately 60 MPa), with a different behavior concerning the effect of the confinement factor. The percentage of silica fume was different in the studies, 5% in [9,10] and 24% in [5]. The results in [11] were obtained by conducting experiments on circular sections constructed using concrete with a compressive strength of 56, 66, and 107 MPa. Coarse aggregate of size 10 mm and fine aggregate were added to the concrete composition. Silica fume was not added. Figure 6 depicts the relationship between the strength index and the confinement factor for the tests conducted in [11]. The strength index increased with an increase in the confinement factor for the different values of concrete compressive strength. The smallest increments in strength corresponded to the highest-compressive-strength concrete. Different experimental results [5,12] were used for an analysis of the effects of the cross-section type on the mechanical behavior of CFSTs. The experimental tests conducted in [12] only used UHSC, in contrast to the results obtained in [5], in which the concrete compressive strength was varied in the range of

60–130 MPa. According to the results, whether the sections were circular or square did not affect the strength index values. However, the utilization of different cross sections resulted in different modes of failure.

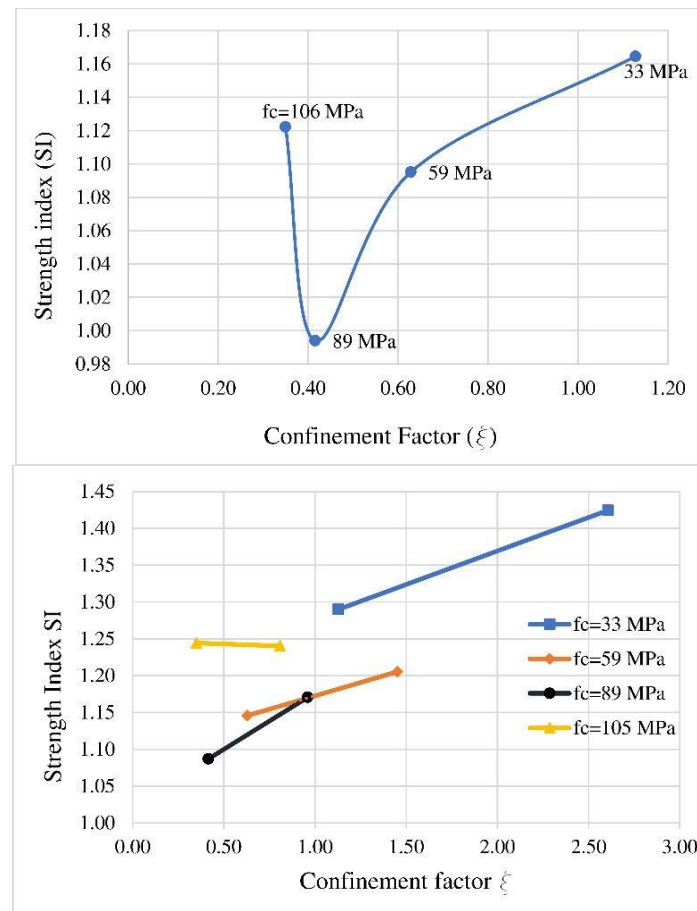


**Figure 5.** Relation between the strength index (SI) and the confinement factor ( $\xi$ ), according to the results of [9] (top) and [10] (bottom),  $L = 3D$ .

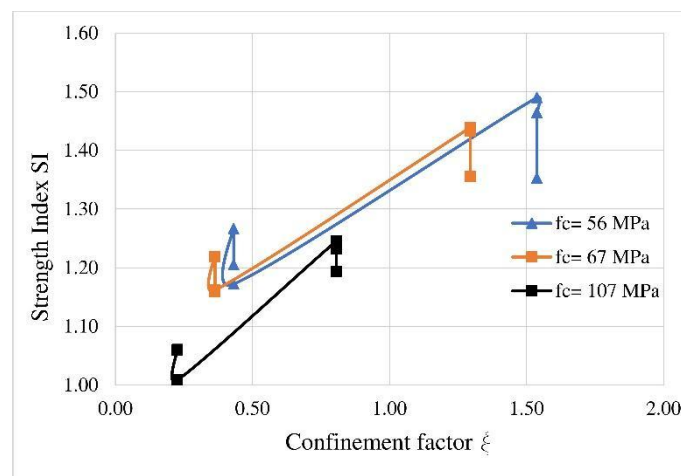


**Figure 6.** Relation between the strength index (SI) and the confinement factor ( $\xi$ ), according to the results of [11].

## 2.2. Failure Modes

The experimental tests conducted on circular CFST elements exhibited four different types of failure modes: (i) failure in the inclined planes (Figure 7); (ii) the formation of bulges (Figure 8); (iii) global buckling of the element (Figure 9); and (iv) local buckling of the steel tube (Figure 10). In the tested circular sections, the transition between the failure in the inclined planes and the formation of bulges was related to an increase in the confinement factor [5]. Conversely, the failure of the square sections occurred with the formation of bulges. The difference between the failure modes of the circular and square sections was confirmed in [8]. The tests were conducted on a concrete specimen with a strength of 111 MPa. The circular sections failed in inclined planes, whereas the square sections failed with the formation of bulges. This demonstrated that the type of cross section affects the failure mode. The failure in circular sections with relatively thin tubes, described in [9,10], occurred in inclined planes. This was also observed for circular sections with high  $L/D$  relations, which were expected to fail via global buckling. The significant increase in tube thickness prevented failure in the inclined planes, leading to failure via the lateral deformation of the tube in the tests with the relation  $L/D = 3$  or via lateral buckling in the tests with the relation  $L/D = 5$  and  $L/D = 7$  (Figure 9). The results in [13] demonstrated the effect of additional external confinement on high-strength-concrete-filled steel tubes (HSCFST) elements. The concrete with a compressive strength of 125 MPa presented an inclined plane of failure inside the steel tube. This result was in contrast to the long axial cracks observed in the unconfined high-strength concrete. The angle of the inclined plane decreased from  $73^\circ$  to  $65.5^\circ$  with an increase in the confinement factor due to the reinforcement of the tube with an outer steel spiral (Figure 11). The values of the compressive strength enhancement were lower than 14%, with a mean value of 7%.

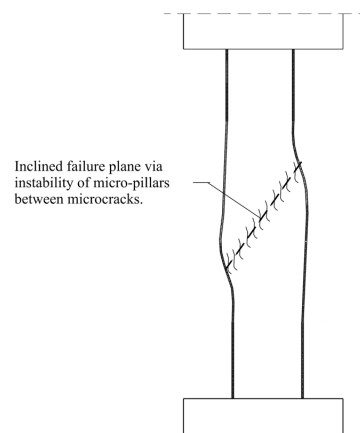


**Figure 7.** Apparent shear failure via instability in an inclined plane ( $L/D = 5$ , based on [9]).

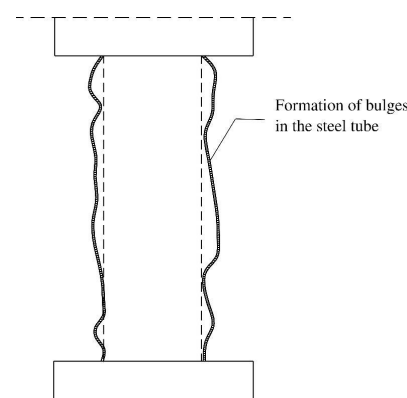


**Figure 8.** Schematic failure mode with the formation of bulges in the tube surface due to the transversal pressure of the internal crushed concrete ( $L/D = 3$ , based on [5]).



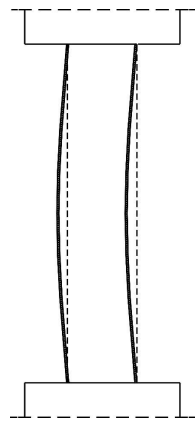


**Figure 9.** Instability with bending via buckling ( $L/D = 5$  and  $L/D = 7$ ), (based on [9,10]).

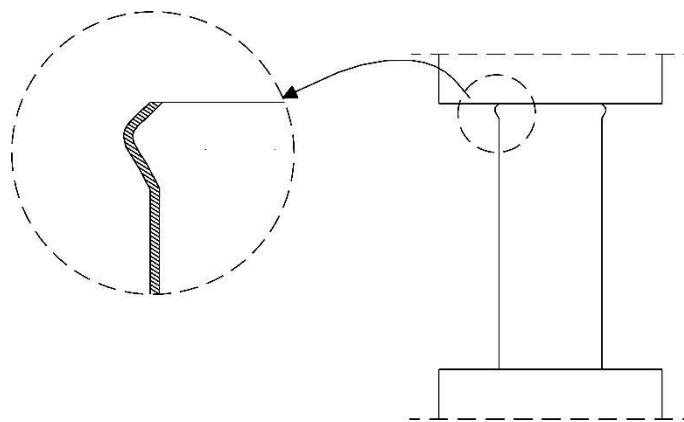


**Figure 10.** Schematic failure mode with local buckling near the ends of the CFST element.

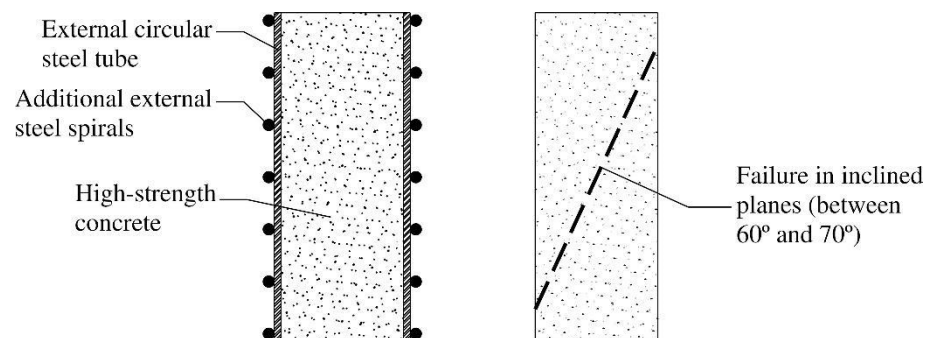


**Figure 11.** CFST specimens with additional external confinement through an external steel spiral and the schematic of the inclined failure plane (based on [13]).

### 2.3. Analysis of the Results

The experimental results demonstrated that it is difficult to establish general principles about the effect of concrete strength or the confinement factor on the load-bearing capacity of CFST elements. Higher values of the strength index were obtained for concrete with a lower compressive strength. However, a distortion in the values was observed at different values of concrete strength. This indicates that the evaluation of the mechanical behavior of CFST elements requires a detailed analysis of the internal destruction processes of concrete and the mechanisms of failure.

The inconsistent results should not be neglected, because understanding them can provide general conclusions about the mechanical behavior of CFST elements. The inconsistency observed in the results was due to the decrease in the strength index (SI) with an



increase in the confinement factor ( $\xi$ ) (Figures 3 and 4), particularly in the case of high-strength concrete. Considering the basic concept of confinement, it should be expected that an increase in the cross section and the tensile strength of the steel tube should increase the compressive strength of the filling concrete.

This fact seems to be not associated with failure in inclined planes, which is not a typical failure mode of HSC in unconfined conditions. According to [19], above a certain value of confining stress (5 MPa), HSC specimens fail with the formation of inclined planes. In confined conditions, the internal damage of the material corresponds to dense and distributed microcracks, instead of long macrocracks. The failure of specimens occurs with the separation of samples into different parts along the weak inclined planes.

According to the abovementioned experimental results, the concept of confinement in CFST elements should be further evaluated. Analyses based on the experimental results for brittle materials such as rocks have presented various similarities to those for CFSTs. A central aspect corresponds to the effect of the steel tube on the internal mechanical destruction of concrete.

### 3. Interpretation of the Mechanical Behavior

#### 3.1. Internal Destruction Processes of Brittle Materials

In the case of uniaxial compression tests of high-strength granite cylinders (height/diameter ratio  $h/d = 2$ ), the measurement of strains and counting the acoustic events (indications of cracking) can enable the detection of the following limits of phases during internal destruction [20,21], (Figure 12): Limit 1: the end of closing of pre-existing microcracks with favorable orientation (non-parallel to the applied loading). Limit 2: the formation of new longitudinal cracks with stable progression. Limit 3: the beginning of the unstable progression of longitudinal cracks. Limit 4 (fgk): failure due to the instability of the pillars or micro-pillars. Limits 2 and 3 can be considered as effective material properties due to their minor dependence upon external factors [22,23]. According to [24], the utilization of similar measurement techniques such as the counting of acoustic events can determine a similar behavior for concrete. Limit 2 occurs at stress values in the range of 0.4–0.5  $f_{ck}$ , and Limit 3 occurs at stress values in the range of 0.75–0.8  $f_{ck}$ . These values are in the range of the values obtained for rocks [20,21,25].

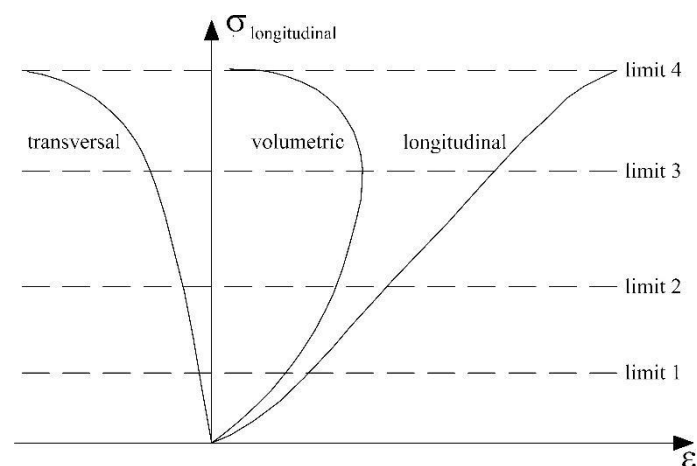


**Figure 12.** Stress–strain curves with the limits between phases of internal destruction (based on [20,23,25,27]).

The similarities between natural rocks and concrete are advantageous because they enable the application of the concepts in field of rock mechanics for the analysis of the mechanical behavior of concrete. Several studies have been conducted on the behavior of high-strength rocks [21–28], such as granites or granodiorites.

These were considered in the present work as references to understand the destruction processes of brittle materials and, consequently, the behavior of CFST elements.

Failure in inclined planes is a relevant aspect of the behavior of compressed brittle materials. Although, failure in inclined planes is similar to that of shear failure, the process does not involve shear processes [20]. The inclined failure planes occur due to the instability of the material as a structural system composed of micro-pillars between cracks [30] (Figure 13), depending upon the crack size, crack density, and loading conditions.

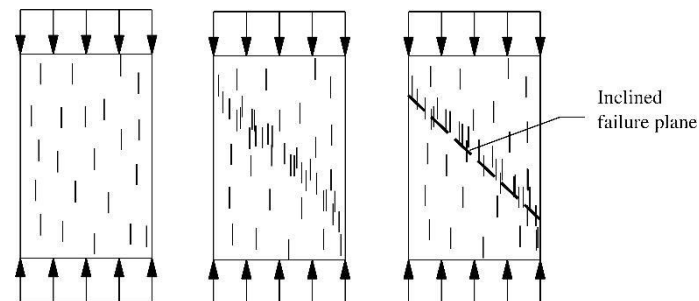


**Figure 13.** Evolution of a crack pattern and formation of an inclined plane of failure in granite under compression (adapted from [30]).

The effect of the steel tube on the filling concrete does not correspond to active confinement, unless some external transversal prestress is used or expansive concrete. The steel tube has a passive effect, which is generated by the internal destruction processes of the concrete corresponding to crack initiation or/and progression.

Moderate transversal confinement is effective for limiting crack progression. However, it has a limited effect on crack initiation [22,24,25]. The concrete inside the steel tube, with passive confinement, corresponds to a system of cracks that can initiate but cannot have significant progression.

The mechanism of crack progression at different levels can be associated with the relative displacement of the irregular crack faces in contact [3]. Therefore, the compressive forces exerted on the faces and the tensile forces exerted on the tips (Figure 14) lead to crack progression [18,35].

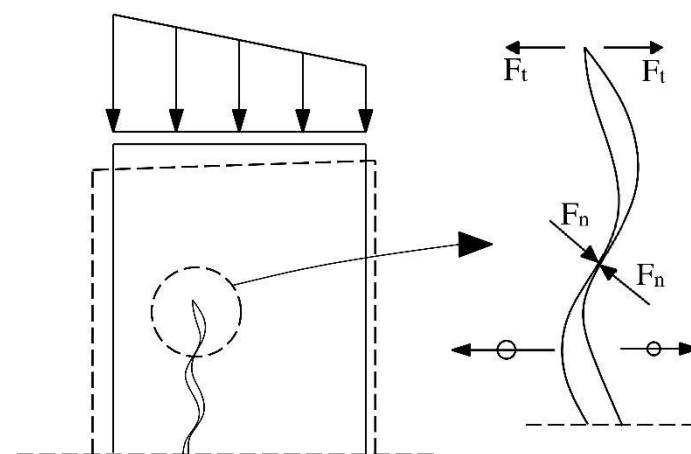


**Figure 14.** Increase in the crack gap due to the relative displacement of the fitted irregular faces ( $F_n$ —force normal to the irregularities in contact;  $F_t$ —tension force at the tips).

The process depicted in Figure 14 and the deformation of the mini-pillars contributes to the mobilization of the steel tube in CFST elements. This has a constraining or bracing effect, instead of an active confinement action. The effect of the steel tube is related to the crack progression because the behavior of damaged concrete is determined by the length, spacing, and distribution of the cracks. These parameters affect the slenderness, spacing, arrangement, and imperfections of micro- or mini-pillars.

According to [24], the cracking process can lead to the confinement of the adjacent zones, where the formation or progression of new cracks is inhibited. For the cases in which the progression of cracks is significant, the resultant longer cracks have an enlarged confinement effect on the adjacent zones (Figure 15). This contributes to a less damaged material. The failure of the resulting structural system occurs via buckling of the mini-pillars (Figures 16 and 17) [20]. Conversely, the limited progression of cracks implies a less enlarged confined adjacent zone (Figure 18), which results in a higher number of distributed cracks and a severely damaged internal system. In this case, an “echelon” of cracks [36] can be formed, with probable failure in inclined planes. Failure of unconfined high-strength brittle materials indicates the formation of long cracks, which are aligned with the applied compression forces. It leads to the separation of specimens in compact pieces [37]. This behavior is observed in conventional short-term compression tests on specimens with dimensions  $h/d > 2$  under monotonic loading. Conversely, the failure mode is different and occurs under loadings lower than those obtained in the conventional tests when the conditions do not permit a higher progression of cracks, such as confinement inside a steel tube.

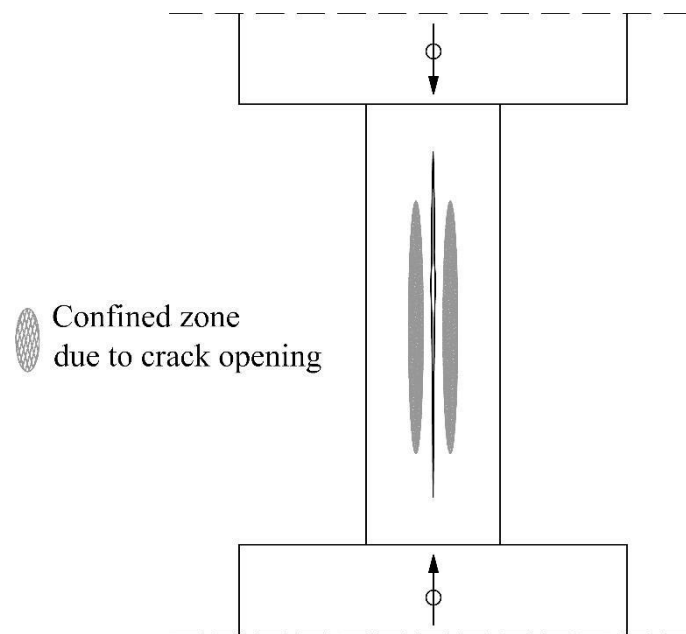


Figure 15. Progression of a long crack inhibiting adjacent cracks.

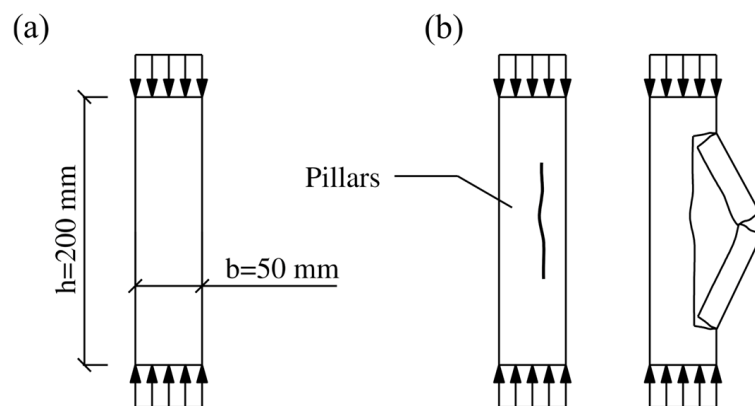
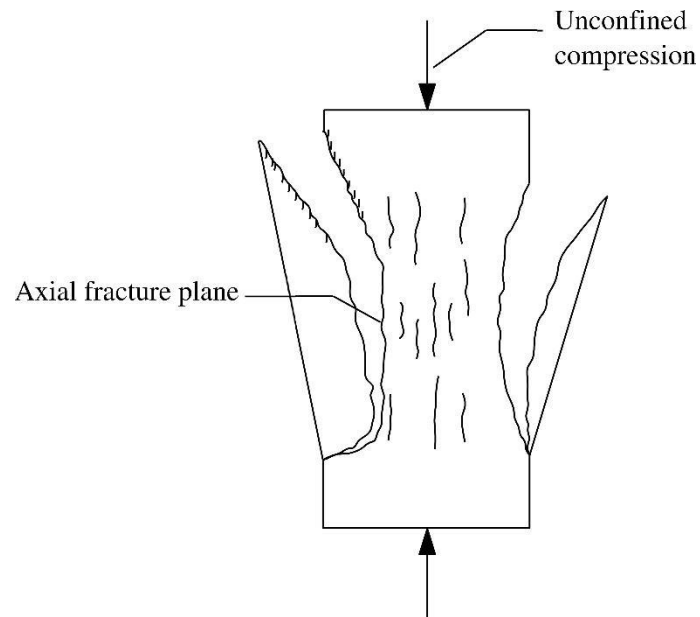
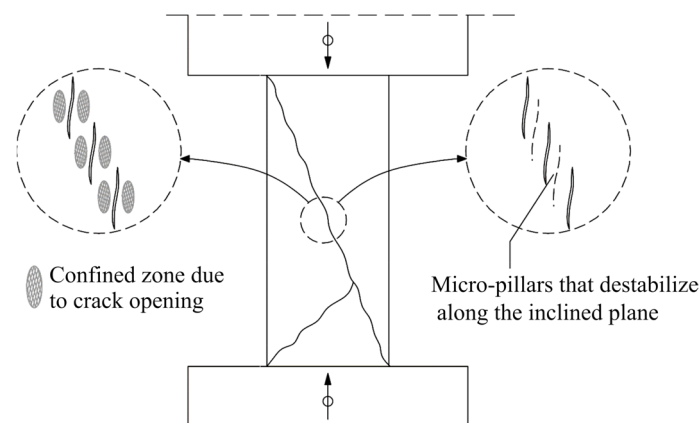


Figure 16. (a) Scheme of a granite prism  $h/b = 4$  under unconfined compression; (b) formation of a macrocrack and failure via the buckling of mini-pillars [37].



**Figure 17.** Failure in unconfined compression with separation in compact pieces after the formation of long cracks and the concentration of small cracks in some zones (adapted from [20]).



**Figure 18.** Failure via global deformation and the simultaneous instability of micro-pillars forming inclined “sliding” planes.

According to [24,26], the application of cyclic loadings at a level that initiates cracks but does not permit their progression implies a degradation in the load-bearing capacity. Conversely, the cumulative internal damage decreases when the cyclic compression loads are sufficient to enable the progression of long cracks. The progression of a few cracks avoids the formation of adjacent cracks (Figure 15). This indicates failure at a higher loading level because the material is internally less degraded and resists the instability of the mini-pillars.

The experimental results presented in [25,28] demonstrated the failure of high-strength granite samples along the inclined planes with “short axial cracks that form adjacent to the failure surface”. This type of failure is not typical in this high-strength material and is related to the test speed because the axial load was applied slowly (0.00075 MPa/s). The failure loading was lower than that obtained in conventional compression tests, in which failure does not occur with the formation of an inclined plane. When the compressive loadings are applied slowly, it inhibits the progression of cracks. The observed behavior with multiple micro-cracks corresponds to the diagram depicted in Figure 18. It does not correspond to Figure 16, which exhibits long cracks. The results of [23,26–28] demonstrated that the conditions of crack progression affect the failure modes and loading capacity. The

factors that prevent crack progression but not their initiation contribute to higher internal degradation and lower loading capacity. Failure with the formation of inclined planes is related to the limited progression of cracks, corresponding to a lower loading capacity [25]. The observations in [25,28] confirmed that the inclined failure plane is a result of specific loading conditions such as the loading rate, without any relation to shear processes.

### 3.2. Effect of Concrete Composition

The composition of concrete affects the cracking pattern of concrete under compressive loads, which affects the behavior of CFST elements. This effect is related to the differences in the behavior between confined and unconfined concrete, in particular, the level of progression and crack density, which determine the behavior of the system in terms of the failure mode and load capacity. For example, in the case of unconfined HSC, silica-fume enhances the progression of cracks, which reduces the density of cracks. The material is globally less damaged and has a high loading capacity. This behavior changes due to the presence of external elements such as steel tubes of fiber-reinforced polymers [38], which can prevent the progression of cracks. However, these elements do not prevent crack initiation. Therefore, it is possible to explain a few of the experimental results reported in Section 2, in which the strength index values decreased with an increase in the confinement factor. This behavior was observed when silica fume was used in the concrete composition without coarse aggregates.

The described behavior is related to the observed failure modes [38] in which the presence of silica fume contributes to failure in the inclined planes of the confined concrete. This type of failure mode, related to the limited progression of cracks is less favorable compared with that of the failure modes observed under unconfined conditions (Figures 16 and 17). The aggregates used in concrete composition led to favorable effects in the strength enhancement of the CFST solutions. The strength and size of the aggregates and the relative strength between the matrix and aggregates affect the cracking pattern. Consequently, this affects the slenderness, distribution, and shape of the micro-pillars (Figure 19). The results obtained in Section 2 (Figures 5 and 6) demonstrated that the presence of aggregates increased the value of the strength index, even using silica fume in HSC composition. Silica fume in HSC with aggregates results in the formation of intragranular cracks, which permits longer cracks and less slender micro-pillars with related favorable effects.

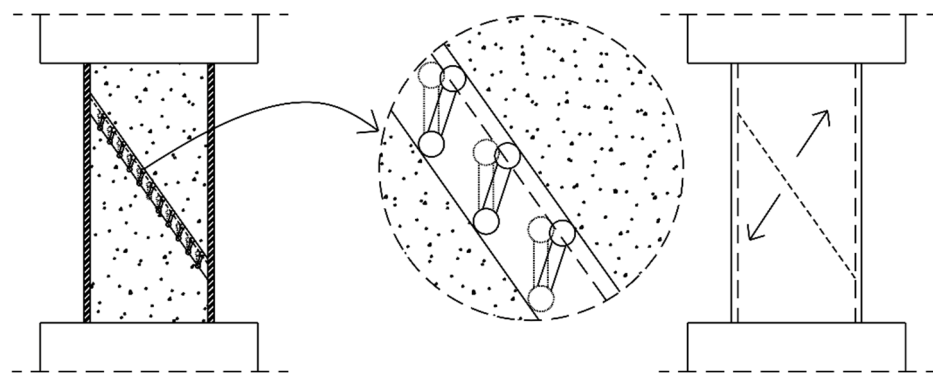


**Figure 19.** Conceptual model for the inclined plane behavior, which generates forces in the tube that determines the interaction between the concrete and the tube.

The effects of steel fibers in the concrete compressive strength based on the results described in [5] were related to the effects of the fibers in the progression of cracks. The analysis considered that the steel fibers enhanced the density of the cracks because their progression was limited (Figures 14 and 15). A superposition of the effects of the steel fibers and the steel tube can exist in a CFST to prevent the progression of cracks and enhance the load-bearing capacity and strength index values.

### 3.3. Composite Effect of HSCFST Elements

The limited progression of cracks due to the steel tube effect constitutes a crucial aspect that relates the behavior of HSCFST elements to the results and analysis presented for high-strength rocks. Although these are different materials, the properties of damaged concrete as a structural system are similar to that of high-strength rocks.

Additional aspects such as shrinkage and low transversal deformability contribute to the low strength enhancement of HSCFSTs. However, these aspects do not explain the reduction in the strength index with an increase in the confinement factor.

Particularly in HSC, with a compact structure, the favorable effect of the steel tube corresponds to a bracing action on the cracked concrete. The confining action is less relevant because the steel tube is passively mobilized. The steel tube contributes to a higher density of microcracks, which promotes failure in the inclined planes and lower relative compression loadings. Therefore, increasing the confinement factor does not always increase the compressive strength of the filling concrete.

The results cited in Section 2 were used for a comparison between the strength index values for circular and square sections. The differences were not significant. The slight differences in the strength index between the two types of sections were not in accordance with the differences based on the theoretical confinement. Circular sections should provide greater confinement than square sections. However, this was not observed for the strength index values. Therefore, it was concluded that the bracing effect of the steel tubes had a greater significance than the confinement effect.

The higher thickness of the circular tubes prevents instability in an inclined plane of the generated system of micro-pillars. Instead of one evident inclined plane, the internal destruction of concrete corresponds to the progressive crushing of micro-pillars, without a significant increase in the compression loadings but with a higher ductile behavior. A consequence of the destruction of the micro-pillars corresponds to the formation of bulges in the tube, as described in [5] (Figure 8).

In square sections, the transversal confinement is generated from the corners with higher effects in the central zone. The distribution of cracks is non-uniform compared with that of circular sections, which affects the mode of failure. The lower uniformity of internal damage leads to worse conditions for failure in inclined planes compared with the circular sections. Additionally, the higher flexibility of the lateral faces enables the local progression of a few cracks, which can have favorable effects.

When the concrete has a greater lateral expansive behavior and a tendency toward the formation of a dense system of micro-pillars under unconfined conditions such as in NSC or low-strength concrete (LSC), the potentially higher confinement effect of circular sections is effectively mobilized. In contrast to compact HSC, the differences between the strength enhancements of circular and square sections are in accordance with the expected confinement action of the two types of sections.

An important aspect in the interaction between concrete and a steel tube is the way that the loading is applied, simultaneously to the concrete and the steel tube or only to the concrete. Experimental studies [39,40] of reinforced concrete columns 2 m in length, strengthened with steel jacketing composed of channels and steel strips, show that it is possible to mobilize the external steel by loading only the concrete, with significant enhancement of the compressive strength. The measurements of the relative displacements between the steel and the concrete show higher values close to the ends and residual values in the middle of the columns. In fact, the steel mobilization occurred in the D-zone [41], with a friction mechanism, observed as a composite action in the B-zone. According to Figure 14, the friction benefits from the transversal pressure generated by the relative displacement of the cracks in a zone where the axial stresses and strains are not uniform.

The experimental tests in [12] enabled evaluation of the effects of loading applied only in the concrete core and simultaneously in the concrete core and in the steel tube. Although the quantitative differences concerning the ultimate loading and compressive strength enhancement were not very significant, it was possible to identify the slip effect



between the tube and the concrete in the confining stresses and in the ultimate compression loading. The friction and the effect of concrete in the external steel elements are well described in [39,40], according to a compression test of normal-strength-concrete square columns, strengthened with steel channels in the corners and steel strips. The relative displacement between the steel and the concrete, the tensile stresses in the steel strips, and the observed effects of the lateral pressure of the concrete on the channels, show a strong interaction between the concrete and the steel. A relevant aspect in these tests corresponds to the dimensions of the tested elements. If the ratio between the height and transversal dimension is higher, it is possible to distinguish D-zones and B-zones. According to Figure 14, the non-uniform distribution of stresses, as expected in the ends of the tested elements [39,40], contributes to higher relative displacements between crack faces, with a higher lateral pressure that mobilizes the friction between steel and concrete. As demonstrated in [39,40], after a length of friction mobilization, the cross section works as a perfect composite. Adequate evaluation of the loading application mode should be made with specimens with higher dimensions, aiming to distinguish the D-zones and B-zones and a minimum distance for friction mobilization.

Based on Figure 14, the parameters that determine the crack pattern, the crack length, and the roughness between their faces will influence the interaction between the concrete and the steel tube. Those parameters depend on the concrete mix, whether there is aggregate or not, the relative strength between the matrix and the aggregate, the aggregate size, the cross-section dimensions, and how the loading is applied.

The idea of the inclined failure being composed of the micro-pillars between cracks also permits a better comprehension of the interaction between the concrete and the tube, explaining, for example, the diagonal fractures in the tubes, as shown in [5,17]. Under compressive loading, the micro-pillars rotate, producing inclined tensile forces in the tube and the observed diagonal fracture. That lateral action creates diagonal tensile stresses in the tube, whose value will depend on the micro-pillars' compressive strength and their length, which inherently are related to the concrete composition and strength. One contribution of this work is the conceptual model shown in Figure 19, which can be developed in future numerical analyses of CFST solutions.

### 3.4. Critical Discussion

The previous subsections discussed the internal destruction processes in concrete that influence the interaction with the external tube. The rock mechanics perspective was chosen based on the similarities with concrete and on the developments in the internal destruction processes. In fact, at this stage, we can understand a conceptual model and a general approach based on the material as a structural system determined by the number, size, and distribution of cracks. This approach is applicable to different materials, including the study of the behavior of CFST elements. The proposed approach was based on an indirect understanding of the failure modes and observations in the tubes, limited by the fact that there were no direct observations in CFSTs, concerning the crack distribution and size. The experimental results were used based on an analogy between rocks and stones. However, future tests are justified to understand the crack pattern in the filling concrete, for example, using acoustic emission counting.

The proposed approach seems to also justify a numerical analysis based on the structural model for the concrete; such an analysis is not compatible with a review paper but is adequate for future work.

## 4. Conclusions

This review introduces a mechanistic approach to the analysis of CFST solutions, based on experimental results and computation models. This approach focuses on the internal destruction processes of brittle materials like natural rocks, with potential contributions for better understanding the interactions between concrete and steel tubes. As this was a review, we did not develop numerical simulations based on the proposed approaches or



the experimental tests with specific conditions. The lack of simulations and tests creates limitations for a deeper analysis; however, it motivates future work on this subject based on the proposed conceptual approaches. The following topics summarize the main conclusions of the review.

- The relationship between the strength index and confinement factor: The strength index (SI) can, in some cases, decrease with an increase in the confinement factor ( $\xi$ ), and the higher compressive strength of concrete tends to result in lower SI values. It is important to understand why increased confinement does not always enhance concrete strength.
- CFSTs' mechanical behavior and structural system: The concept of confinement should be reviewed to better understand the mechanical behavior of concrete-filled steel tubes (CFSTs). Damaged concrete acts as a structural system composed of micro- and mini-pillars, with steel tubes providing bracing during advanced damage phases, enhancing ductile behavior and preventing collapse. This structural system approach is derived from rock mechanics, where the internal destruction processes of brittle materials like natural rocks provide insights into the concrete and steel tube interaction.
- Crack patterns and concrete composition: The density and distribution of cracks significantly affect the strength enhancement and failure modes of CFSTs. Different concrete mixtures, like those with silica fume, can reduce the strength enhancement of CFSTs despite increasing the unconfined compressive strength. Understanding crack patterns in both confined and unconfined conditions is crucial. The idea of concrete as a structural system similar to micro-pillars between cracks forms the basis of this understanding.
- Future directions and a mechanistic approach: There is potential for using high-strength concrete (HSC) and ultrahigh-strength concrete (UHSC) in CFST elements for slender structures. Future research should focus on optimizing concrete mixtures and improving the mechanical interaction between steel and concrete. The proposed mechanistic approach, informed by rock mechanics, can aid in better understanding the interaction between concrete and steel tubes, motivating further experimental and computational studies.

**Author Contributions:** Conceptualization, C.P.; methodology, C.P.; formal analysis, J.F.; writing—original draft preparation, C.P. and J.F.; writing—review and editing C.P. and J.F. All authors have read and agreed to the published version of the manuscript.

**Funding:** This work is supported with Portuguese National Funds BY FCT—Foundation for Science and Technology, I.P. within the C-MADE. <https://sciproj.ptcris.pt/175080UID10.54499/UIDB/04082/2020> (accessed on 22 July 2024).

**Data Availability Statement:** No new data were generated. Data can be accessed through the references in the paper.

**Conflicts of Interest:** The authors declare no conflicts of interest.

## References

1. Zheng, J.; Wang, J. Concrete-Filled Steel Tube Arch Bridges in China. *Engineering* **2018**, *4*, 143–155. [[CrossRef](#)]
2. Han, L.; Li, W.; Bjorhovde, R. Developments and advanced applications of concrete-filled steel tubular (CFST) structures: Members. *J. Constr. Steel Res.* **2014**, *100*, 211–228. [[CrossRef](#)]
3. Shi, J.; Luo, C.; Wang, X. Application of concrete-filled steel tubular arch bridges and study on ultimate load-carrying capacity. *Buildings* **2024**, *14*, 896. [[CrossRef](#)]
4. Abed, F.; AlHamaydeh, M.; Abdalla, S. Experimental and numerical investigations of the compressive behavior of concrete filled steel tubes (CFSTs). *J. Constr. Steel Res.* **2013**, *80*, 429–439. [[CrossRef](#)]
5. Chen, S.; Zhang, R.; Jia, L.; Wang, J.; Gu, P. Structural behavior of UHPC filled steel tube columns under axial loading. *Thin-Walled Struct.* **2018**, *130*, 550–563. [[CrossRef](#)]
6. Wei, J.; Luo, X.; Lai, Z.; Chen, B. Axial compressive behavior of circular UHPC filled high-strength steel tube (UFHST) short columns. In Proceedings of the International Interactive Symposium on Ultra-High Performance Concrete, Albany, NY, USA, 2–5 June 2019.

7. Du, Y.; Chen, Z.; Xiong, M. Experimental behavior and design method of rectangular concrete-filled tubular columns using Q460 high-strength steel. *Constr. Build. Mater.* **2016**, *125*, 856–872. [[CrossRef](#)]
8. Yu, Q.; Tao, Z.; Wu, Y. Experimental behaviour of high performance concrete-filled steel tubular columns. *Thin-Walled Struct.* **2008**, *46*, 362–370. [[CrossRef](#)]
9. Oliveira, W.; Nardin, S.; El Debs, A.; El Debs, M. Influence of concrete strength and length/diameter on the axial capacity of CFT columns. *J. Constr. Steel Res.* **2009**, *65*, 2103–2110. [[CrossRef](#)]
10. Oliveira, W.; Nardin, S.; El Debs, A.; El Debs, M. Evaluation of passive confinement in CFT columns. *J. Constr. Steel Res.* **2010**, *66*, 487–495. [[CrossRef](#)]
11. Ekmekyapar, T.; Al-Eliwi, B. Experimental behaviour of circular concrete filled steel tube columns and design specifications. *Thin-Walled Struct.* **2016**, *105*, 220–230. [[CrossRef](#)]
12. Xiong, M.; Xiong, D.; Liew, J. Axial performance of short concrete filled steel tubes with high- and ultra-high-strength materials. *Eng. Struct.* **2017**, *136*, 494–510. [[CrossRef](#)]
13. Lai, M.; Chen, N.; Ren, F.; Ho, J. Uni-axial behaviour of externally confined UHSCFST columns. *Thin-Walled Struct.* **2019**, *142*, 19–36. [[CrossRef](#)]
14. Berthet, J.; Ferrier, E.; Hamelin, P. Compressive behavior of concrete externally confined by composite jackets. *Part A: Exp. Study. Constr. Build. Mater.* **2005**, *19*, 223–232. [[CrossRef](#)]
15. Ozbakkaloglu, T.; Akin, E. Behavior of FRP-confined normal- and high-strength concrete under cyclic axial compression. *J. Compos. Constr.* **2011**, *16*. [[CrossRef](#)]
16. Vincent, T.; Ozbakkaloglu, T. Influence of concrete strength and confinement method on axial compressive behavior of FRP confined high- and ultra-high-strength concrete. *Compos. Part B Eng.* **2013**, *50*, 413–428. [[CrossRef](#)]
17. Lume, G.J. Mechanical Performance of High Strength Concrete Filled Tubes with High Diameter to Thickness Ratios. Ph.D. Thesis, The University of Sydney, Camperdown, Australia, 2017.
18. Pinto, C.; Fonseca, J. Mechanical behavior of high strength granite for new prestressed stone structures. *Int. J. Rock Mech. Min. Sci.* **2013**, *60*, 452–460. [[CrossRef](#)]
19. Setunge, S.; Attard, M.; Darvall, P. Ultimate strength of confined very high-strength concretes. *ACI Struct. J.* **1993**, *90*, 632–641.
20. Gramberg, J.A. *Non-Conventional View on Rock Mechanics and Fracture Mechanics*; Balkema: Rotterdam, The Netherlands, 1989.
21. Bieniawski, Z. Mechanism of brittle rock fracture: Part I—Theory of the fracture process. *Int. J. Rock Mech. Min. Sci.* **1967**, *4*, 395–406. [[CrossRef](#)]
22. Diederichs, M. Instability of Hard Rockmasses: The Role of Tensile Damage and Relaxation. Ph.D. Thesis, Department of Civil Engineering, University of Waterloo, Waterloo, ON, Canada, 1999.
23. Martin, C. The Strength of Massive Lac du Bonnet Granite around Underground Openings. Ph.D. Thesis, AECL Research, Whiteshell Laboratories, Pinawa, MB, Canada, 1993; 10p.
24. Eberhardt, E. Brittle Rock Fracture and Progressive Damage in Uniaxial Compression. Ph.D. Thesis, Department of Geological Sciences, University of Saskatchewan, Saskatoon, SK, Canada, 1998.
25. Martin, C.; Chandler, N. The progressive fracture of Lac du Bonnet Granite. *Int. J. Rock Mech. Min. Sci.* **1994**, *31*, 643–659. [[CrossRef](#)]
26. Eberhardt, E.; Stead, D.; Stimpson, B. Quantifying progressive pre-peak brittle fracture damage in rock during uniaxial compression. *Int. J. Rock Mech. Min. Sci.* **1999**, *36*, 361–380. [[CrossRef](#)]
27. Hoek, E.; Martin, C. Fracture initiation and propagation in intact rock—A review. *J. Rock Mech. Geotech. Eng.* **2014**, *6*, 287–300. [[CrossRef](#)]
28. Martin, C. The Strength of Massive Lac du Bonnet Granite around Underground Openings. Ph.D. Thesis, Department of Civil Engineering, University of Manitoba, Winnipeg, MB, Canada, 1993.
29. Nguyen, T. Progressive damage of a Canadian granite in laboratory compression tests and underground excavations. *Minerals* **2021**, *11*, 10. [[CrossRef](#)]
30. Hola, J. Studies of failure of high-strength concrete. *Eng. Trans.* **1998**, *46*, 333–351.
31. Yang, W.; Jiang, C.; Wu, Y. Confinement effectiveness of circular concrete-filled steel tubular columns under axial compression. *J. Constr. Steel Res.* **2019**, *158*, 15–27. [[CrossRef](#)]
32. EN 1994-1-1; Eurocode 4: Design of Composite Steel and Concrete Structures-Part 1-1: General Rules and Rules for Buildings. European Committee for Standardization (CEN): Brussels, Belgium, 2004.
33. İpek, S.; Güneyisi, E.M. Application of Eurocode 4 design provisions and development of new predictive models for eccentrically loaded CFST elliptical columns. *J. Build. Eng.* **2022**, *48*, 103945. [[CrossRef](#)]
34. Patel, V.; Hassanein, M.F.; Thai, H.T.; Al Aadi, H.; Elchalakani, M.; Bai, Y. Ultra-high strength circular short CFST columns: Axisymmetric analysis, behaviour and design. *Eng. Struct.* **2019**, *179*, 268–283. [[CrossRef](#)]
35. Jennewein, M. *Zum Bemessen des Stahlbeton mit Stabwerkmodellen*; Institut für Tragwerksentwurf und-konstruktion, Universität Stuttgart: Stuttgart, Germany, 2008.
36. Lajtai, E.; Carter, B.; Duncan, E. En echelon crack arrays in potash salt rock. *Rock Mech. Rock Eng.* **1994**, *27*, 89–111. [[CrossRef](#)]
37. Pinto, C. Design and Structural Analysis of A new Type of Slender Granite Pillar. Master's Thesis Thesis, Department of Civil Engineering and Architecture, University of Beira Interior, Covilhã, Portugal, 2008; 136p. (In Portuguese).

38. Lim, J.; Ozbakkaloglu, T. Influence of silica fume on stress–strain behavior of FRP-confined HSC. *Constr. Build. Mater.* **2014**, *63*, 11–24. [[CrossRef](#)]
39. Giménez, E.; Adam, J.M.; Ivorra, S.; Moragues, J.J.; Calderón, P.A. Full-scale testing of axially loaded RC columns strengthened by steel angles and strips. *Adv. Struct. Eng.* **2009**, *12*, 169–181. [[CrossRef](#)]
40. Giménez, E.; Adam, J.M.; Ivorra, S.; Calderón, P.A. Influence of strips configuration on the behaviour of axially loaded RC columns strengthened by steel angles and strips. *Mater. Des.* **2009**, *30*, 4103–4111. [[CrossRef](#)]
41. Schlaich, J.; Schäfer, K.; Jennewein, M. Toward a consistent design of structural concrete. *PCI J.* **1987**, *32*, 74–150. [[CrossRef](#)]

**Disclaimer/Publisher’s Note:** The statements, opinions and data contained in all publications are solely those of the individual author(s) and contributor(s) and not of MDPI and/or the editor(s). MDPI and/or the editor(s) disclaim responsibility for any injury to people or property resulting from any ideas, methods, instructions or products referred to in the content.